

Comparison of Drainage Line Elements in PLAXIS 2D and 3D applied in Consolidating Marine Clay Deposits

Y.K. Wong, Joseph^{1*}

¹Expert Services / Plaxis AsiaPac Pte Ltd / Singapore

Abstract: This paper compares the performance of drainage line elements available in PLAXIS 2D and 3D, which are finite element coded. The use of 3D eliminates the needs to compute the plane strain's equivalent flow obtained from classical axisymmetric solution. Benchmark testing for a single drainage line element is presented using 2D and 3D against closed form analytical method for radial consolidation. The performance of these drainage line elements are further studied using a well-documented case history, full-scale trial embankment in Muar, West Malaysia, installed with prefabricated vertical drains in the consolidating marine clay deposits. Soft Soil model is applied to describe the highly non-linear behavior of the consolidating material. Predictions of the excess pore pressures dissipation, vertical and lateral displacements are computed and compared with field observation. The studies show that the 3D yields comparable accurate results as of 2D.

Keywords: 2D, 3D, finite element, drain, soft soil, excess pore pressure

1. Introduction

Prefabricated vertical drains (PVD) coupled with surcharge preloading are commonly employed as a ground improvement technique to reduce the excess pore water pressure and stabilize the soft consolidating marine clay. Besides using analytical methods (eg. Barron (1948); Hansbo (1981)), the system could be approached using well-established finite element (FE) procedure which can include modeling the effects of staged construction of the embankment. In reality, the consolidation of soil around a single vertical drain is essentially radial or three-dimensional. However, suggested FE procedures usually idealized the drainage condition in plane strain, computing its equivalent flow. Such methods could be referenced from Hird (1992), Indraratna (1994, 2000, 2005), CUR Publication 191 (1997), etc.

The purpose of this paper presents the choice of 3D modeling, considering with today's relatively cheap and fast computing facilities, as a comparison against 2D analyses. The first part of the paper describes the comparison made with a single line drain element subjected to radial flow in axisymmetric, plane strain and 3D conditions. The second part shall test the features of the drain elements using a well-documented full scale trial embankment, constructed along the North-South Expressway in Muar, West Malaysia by the Malaysian Highway Authority in the 1980s. FE predictions of the excess pore pressures dissipation, vertical and lateral displacements are computed and compared with field

observation, comparing the results obtained from plane strain and 3D.

2. Drainage Line Element in PLAXIS

In PLAXIS 2D, when 15-node soil elements (fourth order) is employed, each drainage line element is defined by five nodes. Whereas when using a 6-node soil elements (quadratic), each drainage line element is defined with three nodes. In PLAXIS 3D, the drainage line element is defined by three nodes when using the 10-node tetrahedral soil elements (quadratic). Relationships between axial force and displacement and axial flow rate and hydraulic gradient are established in the element stiffness matrix. The drainage line elements are assumed having a negligible cross-sectional area in the consolidation analyses.

The drainage line elements, both in PLAXIS 2D and 3D are handled as seepage boundaries and are located inside the domain. At atmospheric pressure, the drains cannot work perfectly and does not permit the discharge of water leaving the domain. Hence, a prescribed head $\bar{\phi}$ should be considered for drain below the water level. The conditions are:

$$\begin{cases} \phi = \bar{\phi} & \text{if outflow} \\ q.n = q_x n_x + q_y n_y + q_z n_z = 0 & \text{if suction} \end{cases} \quad (1)$$

where n_x , n_y and n_z are the outward pointing normal vector components on the boundary and q being the discharge. The drain itself does not generate a resistance against flow.

*Corresponding author: j.wong@plaxis.nl

3. Benchmark Testing

In this section, the validation of the drainage element against closed form solution for radial consolidation given by Barrons (1948) is described. Comparison is made based on studies from 2D axisymmetric, plane strain and 3D models, involving an individual perfect drain in a column of linear elastic soil. The height of the soil column, l is taken as 5m. The effective diameter of the soil column is 1.365m basing on PVD installed at 1.3m spacing in triangle grid, similar to the installed pattern in the latter section. The horizontal permeability is assumed to be 10^{-7} m/s whereas the vertical permeability is considered negligible with a scale down factor of 1,000. Table 1 summarises the input for drain and the soil. In general, the boundary conditions are set to be impervious at the rim of the circumference of the soil column and its base. A nominal surcharge is applied at its top. Depending on the type of analyses, the boundary conditions, where slight adjustment may be made to the effective diameter, are specified and depicted in Figure 1.

Soil

Young Modulus	E'	1×10^5	kPa
Possion Ratio	ν'	0	-
Horizontal Permeability	k_x	1×10^{-7}	m/s
Vertical Permeability	k_y	1×10^{-10}	m/s

Both Hird et al (1992) and Indraratna et al (1997, 2000) have demonstrated in their papers the possibilities of modeling PVD in plane strain analyses where the former introduced a unit cell formulated for plane strain condition by geometric matching. The latter considered multi-drain simulation by adjusting the coefficient of permeability of the soil but maintaining the same rate of consolidation of a converted equivalent parallel drain wall. Both arrived to almost similar equations when ignoring the existence of smear and well resistance as shown in Equation (2) and (3) respectively.

Equivalent horizontal permeability for Plane Strain Condition, Hird et al. (1992)

$$\frac{K_{h,ps}}{K_h} = \frac{0.67}{\left[\ln(n) - \frac{3}{4} \right]} \quad \text{where } n = \frac{d_e}{d_w} \quad (2)$$

Table 1 Inputs for benchmark test
Drain

Description	Sym		Unit
Drain pattern	Triangular		
Drain Spacing	S	1.30	m
Influence-zone diameter	d_e	1.365	m
Diameter of drain	d_w	70	mm

Equivalent horizontal permeability for Plane Strain Condition, Indraratna et al. (2005)

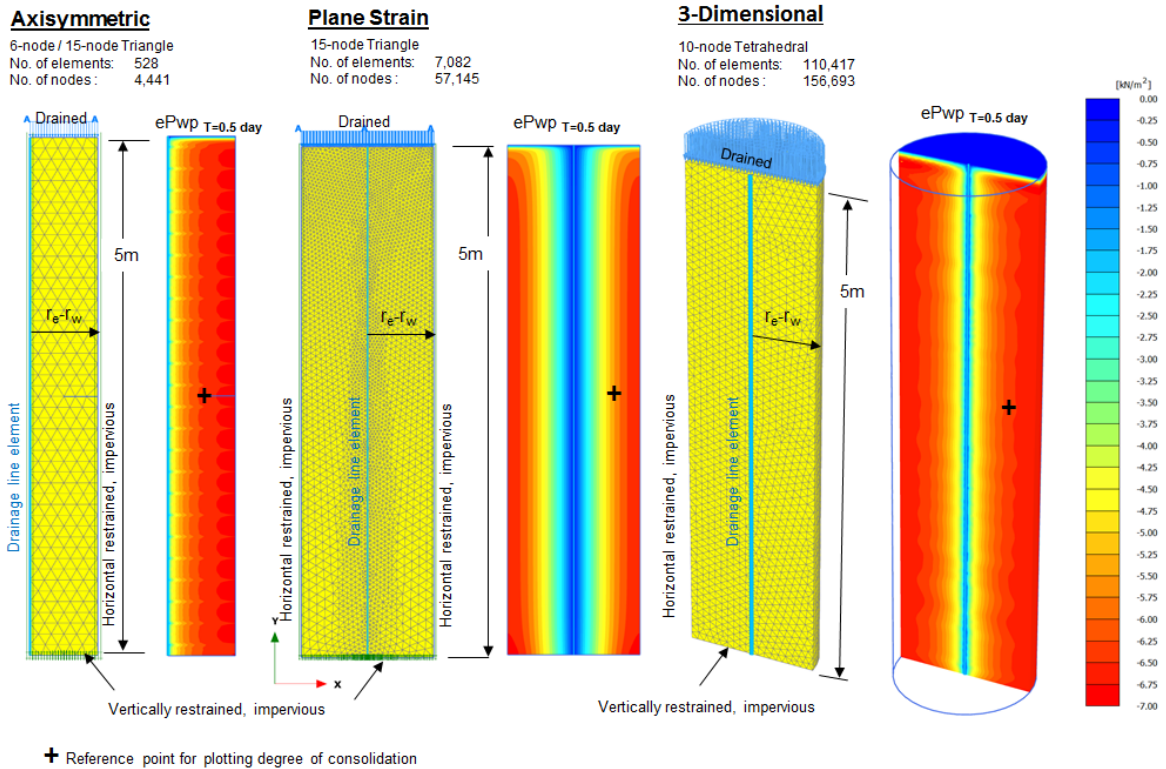


Figure 1 Finite element meshes, boundary conditions and identical excess pore pressure distribution for unit cell axisymmetric, plane strain and 3D.

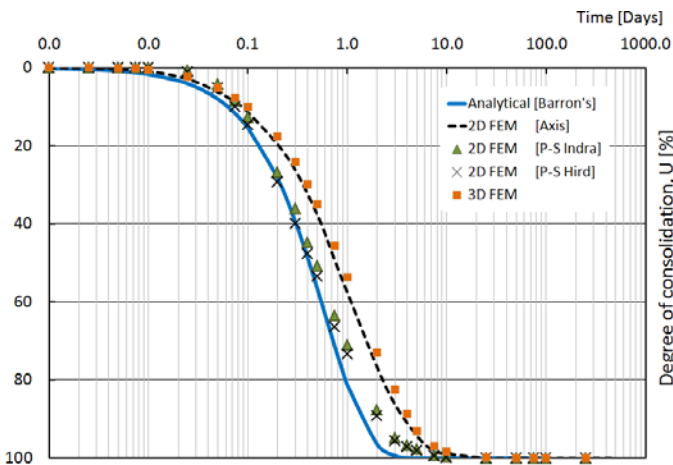
$$\frac{K_{h,ps}}{K_{h,ax}} = \frac{0.67 \frac{(n-1)^2}{n^2}}{\left[\ln(n) - \frac{3}{4} \right]} \quad \text{where } n = \frac{d_e}{d_w} \quad (3)$$

The mesh accuracy in 3D is an order lower than the 2D, 15-node elements, therefore in this benchmark exercise, the author attempts to provide finer mesh discretization in the 3D set-up to avoid the influence of mesh-dependancy to the results. This can be observed in Figure 1 where unusual amount of elements are adopted.

3.1 Results

Figure 2 shows the plot of degree of consolidation against time based on generated excess pore pressure for a single reference at mid-depth and mid-point between the drain and boundary of the soil column (see marked positive signs in Figure 1). The agreement between the FE and analytical solution is generally close. A closer look reveals that the rate of consolidation obtained from 2D axisymmetric and 3D are significantly slower than the analytical and plane strain results. This might suggest that the contact area of the drainage line element in 2D axisymmetric and 3D is lesser (virtual thickness equals to zero) than the surface drain wall in plane strain (2l) and where the analytical solution considered the effective diameter of the drain. Nevertheless, the trend of the degree of consolidation for 3D yields relatively close results with 2D axisymmetric.

Figure 2 Comparison of finite element and analytical solution for consolidation of a unit cell.



4. Application on the Muar Test-Embankment, Malaysia

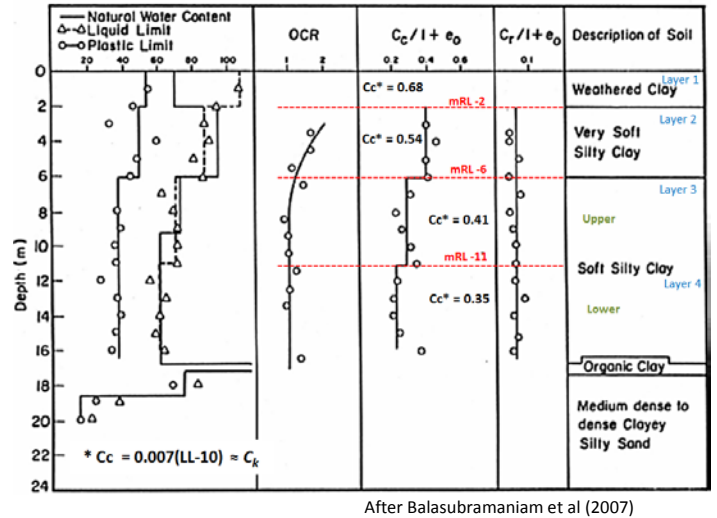
The fully instrumented Muar test embankment conducted in the 1980s is well-suited for the back-

analyses to judge the performance of the drainage line elements which the PVDs were installed at relatively thick layers of the Muar marine clay.

4.1 Soil Conditions at Muar test-site

The stratigraphy of the Muar test-site typically consists a 2m thick weathered crust clay, underlaid with approximately 4m thick of very soft silty clay. Beneath this layer, there seems to exist slightly different properties of the soft silty clay layer which are distinguish as upper and lower layer by the author. The hard founding material is approximately located at 18m depth, overlaid by a thin layer of organic clay which would be ignored in the analyses. The soil profile and the mechanical properties of the soil is shown in Figure 3. In Table 2, the horizontal and vertical permeabilities are calculated based on the results of consolidation tests conducted both vertically and horizontally oriented specimens.

Figure 3 Soil mechanical properties and profile of Muar test-site.



After Balasubramaniam et al (2007)

Table 2 Consolidation and permeability parameters

Depth [m]	Eu ^ [kPa]	ν'^^	Cv ^ [m ² /s]	Ch ^ [m ² /s]	ky [m/day]	kx [m/day]
0 to 2	25500	0.29	7.5E-8	1.0E-7	2.25E-6	3.01E-6
2 to 6	6600	0.31	3.0E-7	4.0E-7	3.24E-5	4.33E-5
6 to 11	9027	0.28	1.4E-7	1.9E-7	1.25E-5	1.72E-5
11 to 18	6239	0.26	1.1E-7	1.5E-7	1.45E-5	2.05E-5

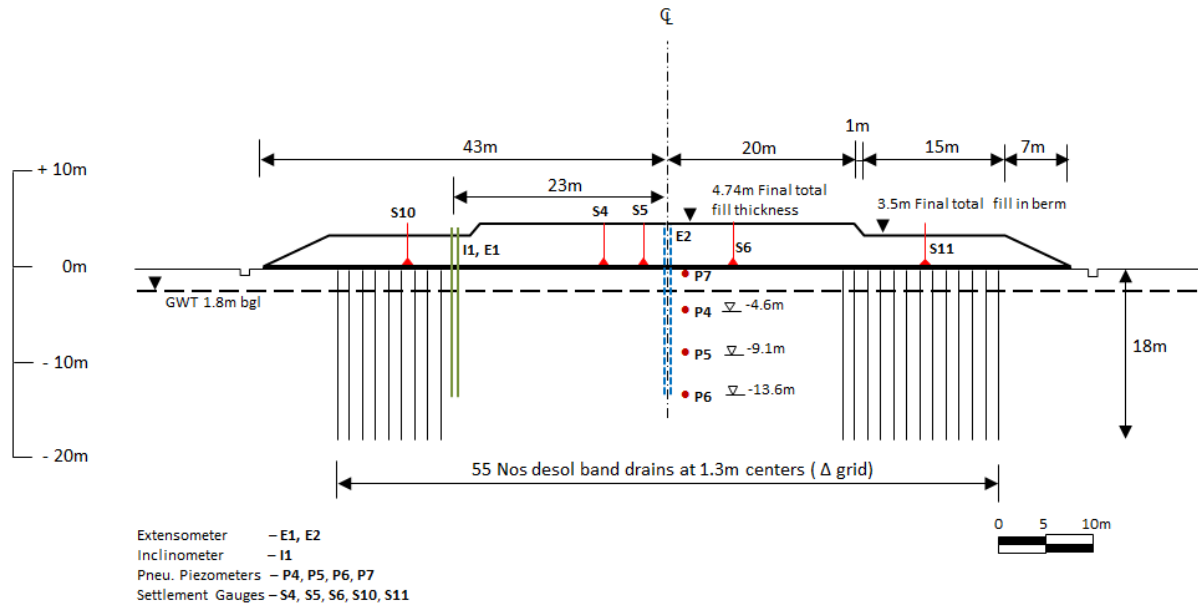
^ After Indraratna et al (1994)

Table 3 Measured and corrected strength parameters

Depth [m]	Measured ^			Corrected (Fail.@20%strain)		
	c' [kPa]	φ' [°]	KoNc	c' [kPa]	φ' [°]	KoNc
0 to 2	8.0	12.5	0.784	5.0	17.0	0.708
2 to 6	14.0	14.0	0.758	3.0	22.0	0.625
6 to 11	15.5	13.5	0.767	3.0	22.0	0.625
11 to 18	15.0	19.3	0.670	7.0	24.0	0.593

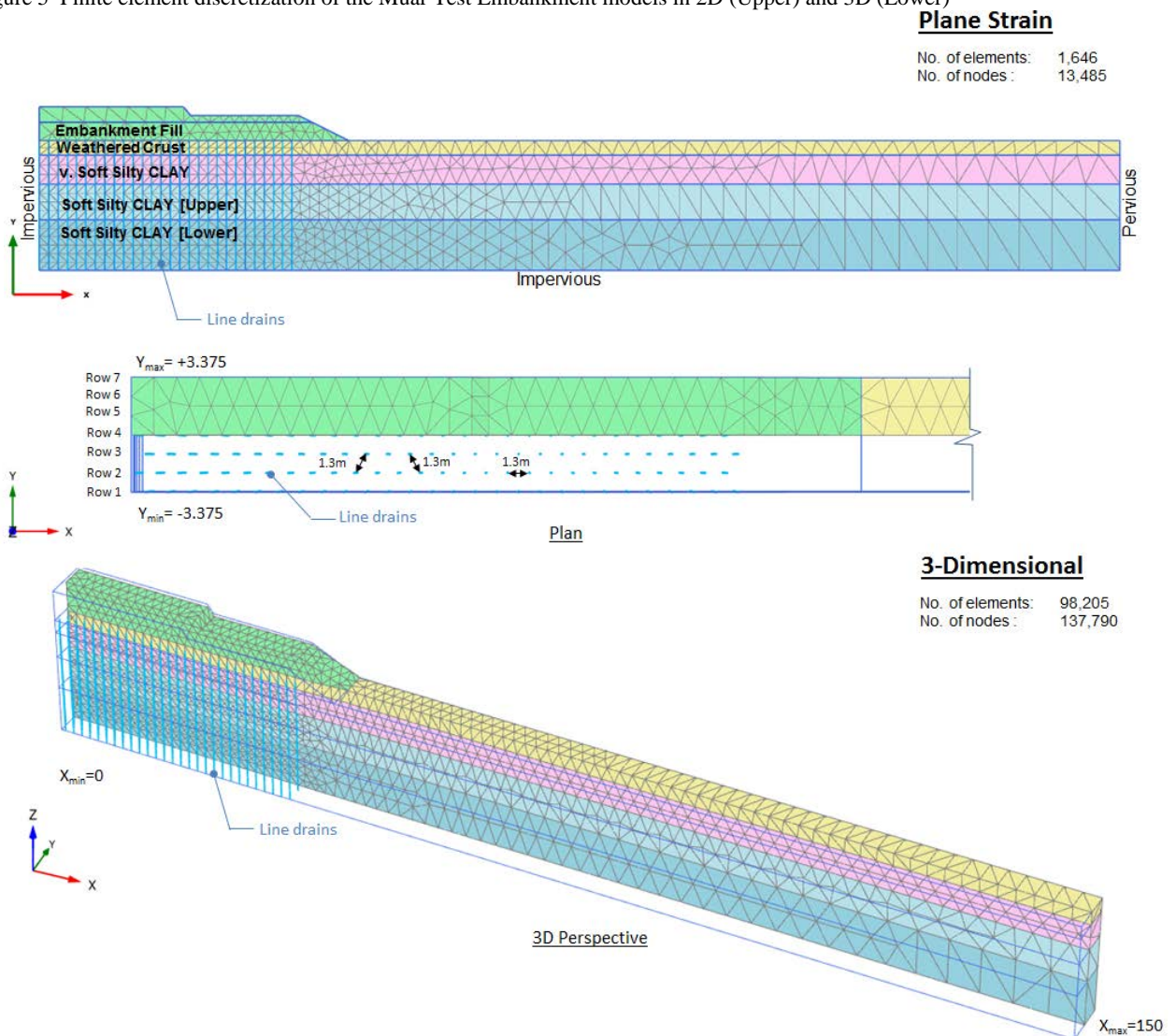
^ After Indraratna et al (1994)

Figure 4 Cross section of the fully instrumented Muar Test Embankment stabilized with PVD



After B. Indraratna et al. (1994), A.S. Balasubramaniam et al. (2007)

Figure 5 Finite element discretization of the Muar Test Embankment models in 2D (Upper) and 3D (Lower)



In the author's opinion, the measured strength parameters from CIU and CID tests are found to be anomalous. Table 3 shows the corrected strength parameter by matching the measured shear yielding and stress paths using the *Soil Test Option* feature in PLAXIS. The obtained strength parameters shown very close resemblance of the strength properties of Singapore marine clay. Furthermore, in the FE initial stress set-up, the generated undrained shear strength profile based on Soft Soil Model with the corrected effective strength parameters corresponds well with the measured Field Vane Shear, undrained shear strengths as shown in Figure 6.

4.2 Layout of fully instrumented test-embankment and FEM Set-up

At the test-site, the clay is treated with PVDs installed at 1.3m spacing in a triangular pattern. The equivalent diameter of each prefabricated drain is 70mm. These PVDs are installed to a depth of 18m below ground level. The embankments were constructed over a period of four months to a height of 4.74m with the primary lift measured at a height of 2.57m, constructed over a period of 14 days and left to consolidate for 90 days. The final lift is constructed over a time period of 24 days. Figure 4 shows the configuration of the test-embankment stabilized with PVDs, together with the layout of the field instruments.

Figure 5 display the FEM set-up for the 2D and 3D model. Since the problem is symmetrical, only one-half of the model is analysed. The impervious hard stratum is assumed to be at 18m below the ground level. The effect of smears and well resistance are not considered in this studies. In the 3D model, a representative slice of the problem was chosen, incorporating 7 rows of drainage line elements to discard any concerns on the boundary's effects.

4.3 Soft Soil Model

Except for the fill materials, the behaviours of the clay layers are described using the advanced constitutive model, Soft Soil Model. This model exhibits a logarithmic compression behaviour with distinction between primary loading and unloading-reloading response. The failure behaviour is in accordance to the Mohr-Coulomb criterion.

The modified compression index, λ^* and modified swelling index, κ^* are essential parameters to describe the logarithmic compression and unloading-reloading behaviours. The λ^* and κ^* differs from the Cam-Clay parameters λ and κ where the former are defined by the volumetric strain, ε_v instead of void ratio, e . The λ^* and κ^* can be obtained from Figure 3 and normalized with a factor of 2.3 defined by the ratio between the logarithm of base 10 and the natural logarithm.

The FE models properties have been summarized in Table 4. The material properties are defined in terms of effective strength and stiffness parameters. Undrained behaviour has also been assumed for all except the fill layer. For the 2D analyses, the equivalent horizontal permeability is applied using Indraratna's equation whereas the actual permeabilities are applied for the 3D analyses.

Table 4 FEM parameter inputs

Identification	Embankment Fill	Weather Crust	v. soft silty CLAY	Soft silty CLAY [Upper]	Soft silty CLAY [Lower]	Unit
<i>General</i>						
Material model	Mohr-Coulomb	Soft Soil	Soft Soil	Soft Soil	Soft Soil	-
Material behaviour	Drained	Undrained	Undrained	Undrained	Undrained	-
γ_{sat}^{\wedge}	20.7	16.5	15.0	15.5	16.0	kN/m ³
e_{init}	0.5	1.82	1.82	0.33	0.14	-
<i>Parameters</i>						
E_{50}	1.00E+5	-	-	-	-	kN/m ²
ν or ν_u	0.25	0.495	0.495	0.495	0.495	-
$\lambda^* \wedge$	-	0.13	0.179	0.122	0.093	-
$\kappa^* \wedge$	-	0.013	0.021	0.025	0.026	-
c_{ref}	14.0	5.0	3.0	3.0	7.0	kN/m ²
$\phi' (\text{phi})$	31	17	22	22	24	°
<i>Flow parameter</i>						
$k_x = k_y$	0.60	3.01E-6	0.043E-3	0.017E-3	0.021E-3	m/day
k_z	0.60	2.25E-6	0.032E-3	0.012E-3	0.015E-3	m/day
$k_h \#$	-	8.17E-7	1.17E-5	4.66E-6	5.58E-6	m/day
c_k	1.0E+15	0.68	0.54	0.41	0.35	-
<i>Initial</i>						
OCR^{\wedge}	1.0	1.8	1.5	1.0	1.0	-

[^] After Indraratna et al (1994) & Figure 3

[#] Derived from Equation (3)

4.4 Change of permeability, c_k

This advanced feature built in PLAXIS is to account for the change of permeability during a consolidation analysis. The permeability will change according to the following relationship:

$$\log\left(\frac{k}{k_0}\right) = \frac{\Delta e}{c_k} \quad (4)$$

where Δe is the change in void ratio, k is the permeability in the calculation and k_0 is the input permeability. Since the c_k -value is generally in the order of the compression index C_c , the values are computed based on the following relationship with liquid limit:

$$C_c = 0.007(LL - 10) \approx C_k \quad (5)$$

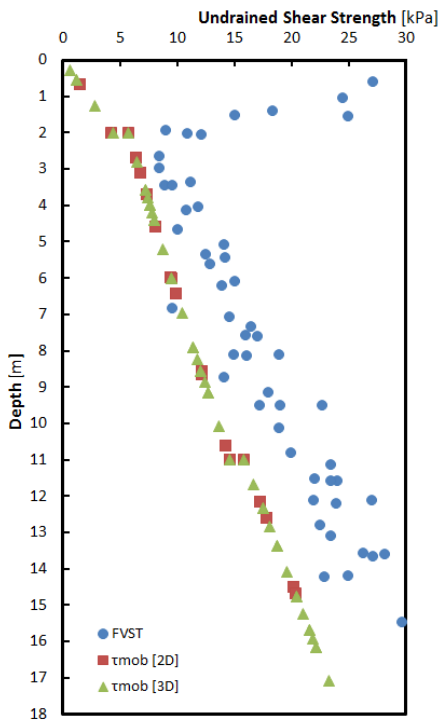
The c_k -value will have an influence on the rate of consolidation as will be discussed in the later section.

4.5 Calculation Phases

The following construction phases have been defined for the FE analyse:

- Phase 0: Initial Stress (K_0 -procedure)
- Phase 1: PVD Installation (Plastic Analysis)
- Phase 2: Preload to mRL +2.57 at a period of 14 days
- Phase 3: Consolidate over 90 days
- Phase 4: Preload to mRL +4.74 at a period of 24 days
- Phase 5: Consolidate over 222 days

Figure 6 Undrained Shear Strength Profile, Measured against FE generated



4.5 Numerical Prediction

Figure 7 presents the time-dependent excess pore pressure variations along near-centerline of the embankment. Two pneumatic piezometer readings were available, P5 (at -9.1m) and P6 (at -13.6m). The excess pore pressure predictions are generally acceptable although higher readings are computed at the lower soft silty clay layer for both the 2D and 3D. The dissipation of the excess pore pressure in the FE analyses were much faster than the measured data as perfect drain conditions are present where in reality, the actual drains may be clogged, coupled with smear-zone during installations. In general, the computed 3D results are generally lower than the 2D probably due to the smaller contact area of the drainage line element as discussed earlier in Section 3.

As shown in Figure 8, the prediction of surface settlements from both the 2D and 3D has very good

agreements with the field measurements. However, at greater depths, the subsoil settlements are larger than field measurements and could be explained with increasing stiffness at deeper depth where the Soft Soil Model may not capture well on the highly non-linear response of the Muar Clay. Nevertheless, 2D and 3D yields similar surface and subsoil settlement results.

One may noticed that if the default c_k -value are adopted for the soft clay layers, the rate of consolidation would be rapid and the settlements would be occurred at a very much earlier time period due to perfect drain conditions. Therefore, it is important to include the proper c_k -value to estimate the consolidation response of the site. From the results, it can be concluded that the compression index obtained from equation 5 can be applied to estimate the rate of consolidation for the Muar Clay.

Figure 7 Excess Pore Pressure Distribution against Time

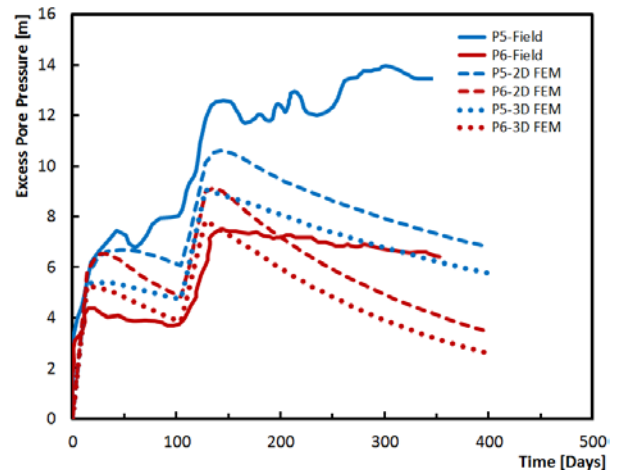


Figure 8 Comparison of surface and subsoil settlements at the Centerline of the Embankment

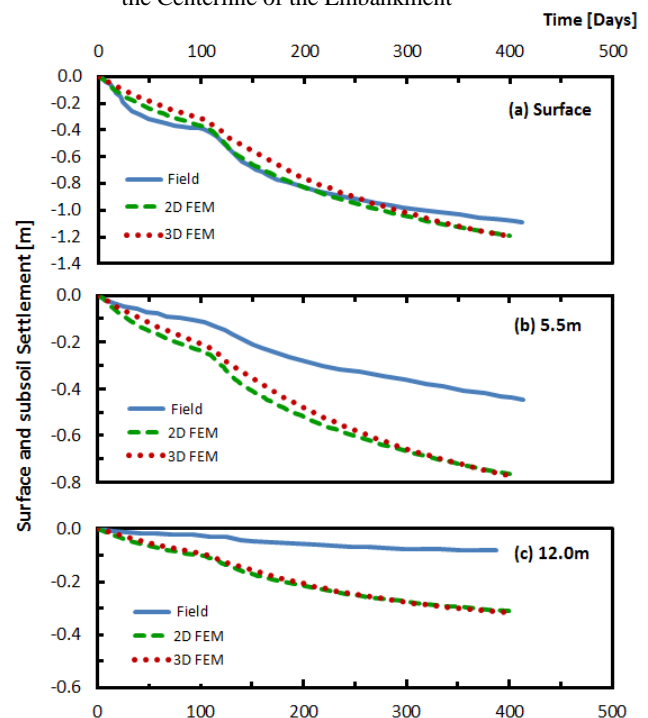


Figure 9 Settlement contours at ground level at stipulated time period

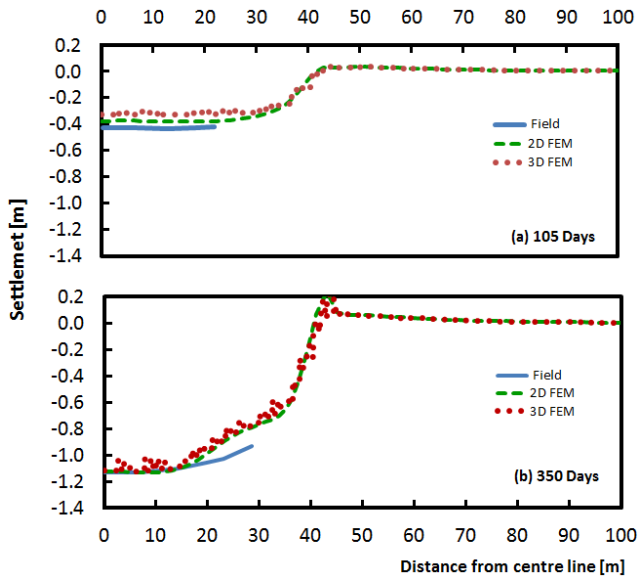
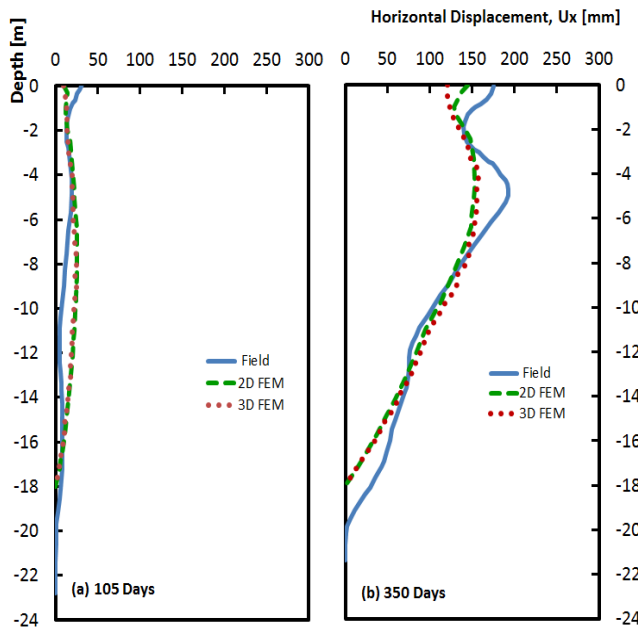


Figure 10 Horizontal displacements at Inclinerometer location (23m from Centerline)



Both 2D and 3D shows very similar ground settlements contours at time period 105 days and 350 days. The FE computations are in very good agreement with the field measurements as shown in Figure 9.

The prediction of lateral deformation is shown in Figure 10. Both 2D and 3D slightly over-predicted the lateral deformation at depth between 6 to 14m at time period 105 days. However, at time period 350 days, the FE slightly underestimate the lateral deformation near the ground surface. The field data shows larger

deflection occurred at the toe due to the inclinometer is not considered entirely fixed as of the model set-up.

Figure 11 Excess pore pressure coloured contour plot for 3D FE analysis at 105 days and 350 days

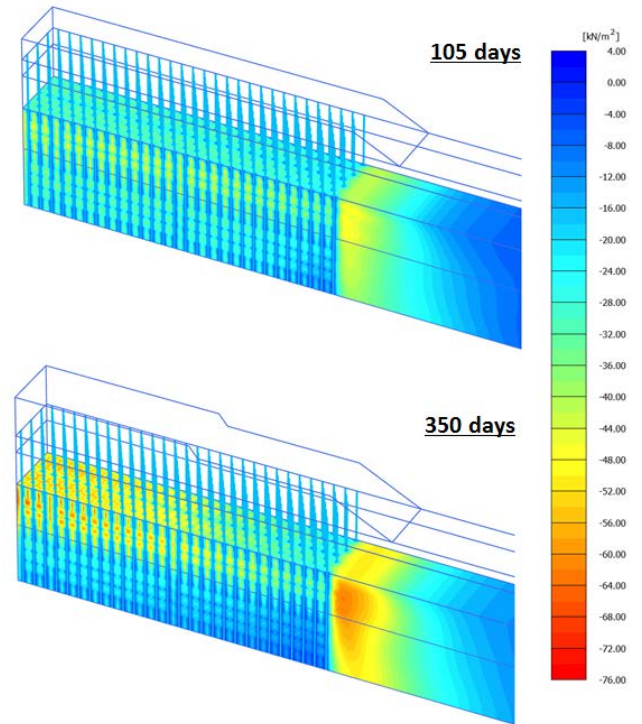


Figure 12 Total displacement shaded contour of the test-embankment in 3D at 350 days

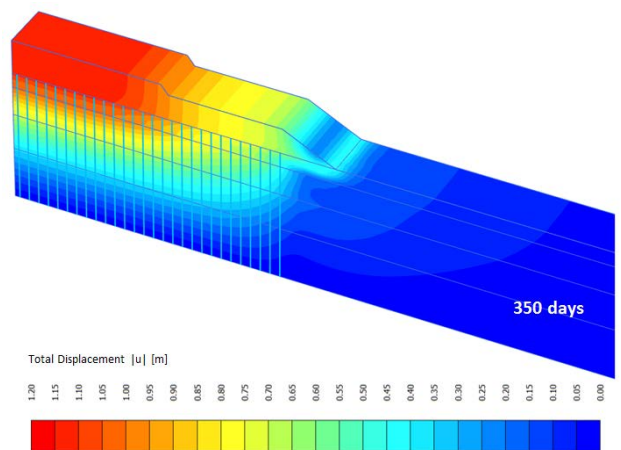


Figure 11 shows the 3D's output for the excess pore pressure distributions at two different time period. Only in 3D, one can view the radial consolidation within the drainage line elements whereas this is not possible to view in plane strain mode. Figure 12 shows the possible total displacements and its displacement

contours at time period 350 days, expressing the mode of deformation the embankment undergoes.

5. Conclusions

In the benchmark tests, the 3D analyses have demonstrated that it gives relatively close degree of consolidation's trend with 2D axisymmetric, though it does not consider the effective diameter of the physical PVD.

Although the PLAXIS 3D uses quadratic elements and is considered less accurate than the fourth order elements presents in PLAXIS 2D, the studies show that the performance of drainage line elements in 3D yields almost similar results as of 2D and vice versa, and also in good agreement with the field data for the real application. Hence, the user can also directly input the PVD patterns in the 3D model without considering the needs to compute the equivalent flow in 2D and its geometric consideration.

The advanced constitutive model, Soft Soil model describes well with the behavior of Muar clay. The consideration of the use of change in permeability is essential to predict the rate of consolidation.

Acknowledgements

The author would like to thank Balasubramaniam, A.S. (Griffith University, Australia) for the technical sharings and Harry Tan, S.A. (National University of Singapore, Singapore) for some useful insights and the development of this paper. The author would also like to extend his thanks to his colleagues, Ronald Brinkgreve and Vahid Galavi for their valuable comments and also the committees of SEIC'13 for their invitation of this paper write-up.

References

[1] Balasubramaniam, A.S. et al. Interpretation and analysis of test embankments in soft clays with and without ground improvement. *Journal of the*

Southeast Asian Geotechnical Society. (2007), pp. 235-254.

- [2] *CUR-Publication 191*; Achtergronden bij numerieke modellering van geotechnische constructies, Deel 2 (1997)
- [3] Hansbo, S. Aspects of vertical drain design: Darcian and non-darcian flow. *Géotechnique* 47, No. 5, (1997), pp. 983-992.
- [4] Hird, C.C., Pyrah, I.C., Russell, D. Finite element modeling of vertical drains beneath embankments on soft ground. *Géotechnique* 42, No. 3, (1992), pp. 499-511.
- [5] Indraratna, B., Balasubramaniam, A.S., Balachandran, S. Performance of test embankment constructed to failure on soft marine clay. *International Journal of Geotechnique Engineering*, 118(1), (1992), pp. 12-33.
- [6] Indraratna, B., Balasubramaniam, A.S., Ratnayake, P. Performance of embankment stabilized with vertical drains on soft clay. *International Journal of Géotechnique Engineering*, 120(2), (1994), pp. 257-273.
- [7] Indraratna, B., Salim, W., Redana, I.W. Predicted and observed behavior of soft clay foundations stabilized with vertical drains. *GeoEng2000, An International Conference on Geotechnical & Geological Engineering*, Vol 1, (2000).
- [8] Indraratna, B., Rujikiatkamjorn, C., Sathananthan, I., Analytical and numerical solutions for a single vertical drain including the effects of vacuum preloading. *Canadian Geotechnical Journal*, No. 42. (2005), pp 994-1014.
- [9] PLAXIS 2D User's Manuals (2010), Edited by Brinkgreve, R.B.J., Swolfs, W.M. and Engin, E., Plaxis BV, Delft, The Netherlands
- [10] PLAXIS 3D User's Manuals (2012), Edited by Brinkgreve, R.B.J., Swolfs, W.M. and Engin, E., Plaxis BV, Delft, The Netherlands